**INTERNATIONAL JOURNAL OF OPTIMIZATION IN CIVIL ENGINEERING**
***Int. J. Optim. Civil Eng., 2020; 10(4):595-609***

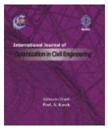

# EVALUATION THE EFFECT OF STRONG COLUMN-WEAK BEAM RATIO ON SEISMIC PERFORMANCE OF OPTIMALLY DESIGNED STEEL MOMENT FRAMES

A. Nabati and S. Gholizadeh[*, †]
*Department of Civil Engineering, Urmia University, Urmia, Iran*

## ABSTRACT

The present work is aimed at assessing the impact of strong column-weak beam (SCWB) criterion on seismic performance of optimally designed steel moment frames. To this end, different SCWB ratios are considered for steel special moment resisting frame (SMRF) structures and performance-based design optimization process is implemented with the aid of an efficient metaheuristic. The seismic collapse performance of the optimally designed SMRFs is assessed by performing incremental dynamic analysis (IDA) and determining their adjusted collapse margin ratios. Three design examples of 5-, 10-, and 15-story SMRFs are presented to illustrate the efficiency of the proposed methodology.

**Keywords:** metaheuristic structural optimization; strong column-weak beam rule; performance-based design; seismic collapse performance; steel moment frame.

Received: 20 August 2020; Accepted: 25 October 2020

## 1. INTRODUCTION

One of the reliable lateral load resisting systems in seismic prone zones is steel special moment resisting frames (SMRFs). For SMRFs the seismic energy dissipation capacity significantly depends on the flexural yielding of the beam ends rather than that of the column ends. A story mechanism can be occurred due to extensive plastic hinging of columns in a story and this results in dynamic instability [1]. In order to reduce the likelihood of forming a story mechanism and to ensure the ductility capacity of SMRFs, the strong-column weak-beam (SCWB) criterion has been suggested by AISC [2]. Based on this criterion if in a beam-to-column structural joint, the ratio of flexural strength of the columns is increased to that of the beams, the probability of the plastic hinges formation in the columns will be reduced and spreading of plasticity will be shifted to the ends of beams [3].

---

[*]Corresponding author: Department of Civil Engineering, Urmia University, Urmia, P.O. box 165, Iran
[†]E-mail address: s.gholizadeh@urmia.ac.ir (S. Gholizadeh)

According to the SCWB criterion, at beam-to-column joints, the summation of the flexural strengths of the columns must be greater than that of the beams. This criterion can generally be expressed in the form of

$$\frac{\sum M_{pc}}{\sum M_{pb}} \geq FS \tag{1}$$

where $\sum M_{pc}$ and $\sum M_{pb}$ are respectively sum of the plastic flexural strengths of columns and beams connected at a beam-to-column joint; and $FS$ stands for factor of safety. AISC [2] suggested $FS = 1$ for SMRFs however different values have been suggested in literature [3-5] for inducing the beam–hinge mechanism. It has been demonstrated that increasing $FS$ increases the seimic collapse capacity of SMRFs [6].

Performance-based design (PBD) [7] is a modern seismic design procedures for the rehabilitation of existing structures and the seismic design of new ones. In the framework of PBD structural seismic response should be evaluated by structural nonlinear analysis and therefore its computational effort is more than that of elastic design process. One of the major concerns of structural designers is to find cost-efficient structures having acceptable performance subject to earthquake. For this purpose, structural optimization methodologies have been developed in the last decades and structural performance-based optimal design (PBOD) becomes a topic of growing interest [8-17] in the field of structural engineering. In order to deal with PBOD problems, it is necessary to use global search algorithms such as metaheuristics. Metaheuristics are designated based on stochastic natural phenomena and they have attracted a great deal of attention during the last two decades. As the metaheuristic optimization techniques require no gradient computations, they are simple for computer implementation. During the recent years, researchers have designed many metaheuristic algorithms and many successful applications of them have been reported in optimization literature. In the current study, center of mass optimization (CMO) [18] is applied to solve PBOD problem of SMRFs because its ability for tackling PBOD problems of steel structures have been demonstrated in the previous studies [18-20].

Seismic collapse capacity of structures is one of the most important concerns of structural engineers. In order to determine the seismic safety factor of structures, collapse fragility curves must be developed by performing incremental dynamic analysis (IDA) [21] for a prescribed set of ground motions whose amplitudes are scaled to reflect specified earthquake intensities. Subsequently, the collapse margin ratio (CMR) of structures can be determined based on the methodology of FEMA-P695 [22] provided for quantifying building system performance in the context of collapse safety.

This study is focused on evaluating the effect of beam to column strength ration $FS$ on the seismic collapse safety of optimal steel SMRFs designed in the context of PBD. Three illustrative design examples of 5-, 10-, and 15-story steel SMRFs are presented. For each design example, four values of 1.0, 1.25, 1.5, and 2.0 are taken for $FS$ and three independent optimization runs are implemented for each case by using CMO metaheuristic algorithm. The confidence level of the structures at performance levels are checked during PBOD process as the design constraints in accordance with FEMA-350 [23]. Finally, the seismic collapse safety of the optimal designs are assessed using the methodology of FEMA-P695.

## 2. PERFORMANCE-BASED OPTIMUM DESIGN

According to the philosophy of PBD approach, the structures should meet performance objectives for a set of hazard levels. FEMA-350 divided performance ratings into two levels: Immediate Occupancy (IO), and Collapse Prevention (CP). The IO level implies very light damage with minor local yielding and negligible residual drifts, while the CP level is associated with extensive inelastic distortion of structural members with little residual strength and stiffness. FEMA-350 defined two hazard levels including earthquakes with 50% and 2% probability of exceedance in 50 years. Geometric and strength constraints should be checked prior to seismic performance checking. In other words, geometric constraints should be checked at each structural joint to ensure that the dimensions of beams and columns are consistent. As the strength constraints, the strength of structural members need to be checked for gravity loads based on AISC 360-16 [24]. If these constraints are satisfied, nonlinear structural analysis is performed for checking PBD constraints. Based on provisions of FEMA-350, the constraints of confidence level (CL) at IO and CP performance levels can be written as follows:

$$\frac{CL_{PL}}{\overline{CL}_{PL}} - 1 \geq 0 \, , PL = \mathrm{IO, CP} \tag{2}$$

where $\overline{CL}_{PL}$ for IO and CP performance levels are 50% and 90% which are correspond to 1.0673% and 5.9385% inter-story drift ratios, respectively.

The confidence level for hazard levels can be computed using the following equation:.

$$CL = \emptyset\left(\frac{k\beta_{UT}}{2} - \frac{ln\left(\frac{\gamma\gamma_a D}{\varphi C}\right)}{\beta_{UT}}\right) \tag{3}$$

in which $\emptyset$ is the normal cumulative distribution function; $k$ is the slope of the hazard curve; $\beta_{UT}$ is an uncertainty measure; $\gamma$ is a demand variability factor; $\gamma_a$ is an analysis uncertainty factor; $D$ is the calculated demand; $C$ is the capacity; and $\varphi$ is a resistance factor [23].

In this work, pushover analysis is conducted to evaluate the structural nonlinear responses. In this method, the structure is pushed with a specific distribution of lateral loads, until the displacement of a specific point of the structure reaches the target displacement. The PBOD problem of steel SMRFs can be formulated as follows:

$$\text{Minimize: } f(X) = \sum_{i=1}^{ne} \rho_i L_i A_i \tag{4}$$

$$\text{Sobjec to: } g_j(X) \leq 0 \, , j = 1, \ldots , nc \tag{5}$$

where $X$ is a vector of design variables; $f$ is the structural weight; $\rho_i$, $L_i$, and $A_i$ are weight density, length and cross-sectional area of the $i$th element, respectively; $g_j$ is the $j$th design constraint; and $nc$ is the number of design constraints.

## 3. CENTER OF MASS OPTIMIZATION

CMO was proposed in [18] based on the concept of center of mass in physics. In CMO algorithm, a population including $np$ randomly selected particles $(X_i\ , i \in [1,np])$ is generated in design space. The mass of $i$th particle $m_i$ is determined as follows

$$m_i = \frac{1}{f(X_i)} \tag{6}$$

Particles are sorted based on their mass values in ascending order and then they are equally divided into two groups of G1 and G2. The first half of particles are put in G1 and the others in G2. The particles in G1 are paired with their corresponding ones in G2. The position of center of mass and the distance between $j$th ($j$=1,..., $np/2$) pair of particles in iteration $t$ are determined as follows

$$X_j^C(t) = \frac{m_j X_j(t) + m_{j+\frac{np}{2}} X_{j+\frac{np}{2}}(t)}{m_j + m_{j+\frac{np}{2}}} \tag{7}$$

$$d_j(t) = \left| X_j(t) - X_{j+\frac{np}{2}}(t) \right| \tag{8}$$

In order to switch between exploration and exploitation of CMO algorithm, the following parameter is computed in which $t_{max}$ is the maximum number of iterations.

$$CP(t) = \exp\left(-\frac{5t}{t_{max}}\right) \tag{9}$$

The position of $j$th couple of particles is updated using the following equations

$$if\ d_j(t) > \ CP(t) \tag{10}$$

$$X_j(t+1) = X_j(t) - R_1\left(X_j^C(t) - X_j(t)\right) + R_2\left(X_b - X_j(t)\right) \tag{11}$$

$$X_{j+\frac{np}{2}}(t+1) = X_{j+\frac{np}{2}}(t) - R_3\left(X_j^C(t) - X_{j+\frac{np}{2}}(t)\right) + R_4\left(X_b - X_{j+\frac{np}{2}}(t)\right) \tag{12}$$

$$if\ d_j(t) \leq \ CP(t) \tag{13}$$

$$X_j(t+1) = X_j(t) + R_5\left(X_j^C(t) - X_{j+\frac{np}{2}}(t)\right) \tag{14}$$

$$X_{j+\frac{np}{2}}(t+1) = X_{j+\frac{np}{2}}(t) + R_6\left(X_j^C(t) - X_{j+\frac{np}{2}}(t)\right) \tag{15}$$

where $R_1$ to $R_6$ are vector of random numbers in [0,1]; and $X_b$ is the best solution found.

There is a mutation operator in CMO to decrease the probability of local optima entrapment. A mutation rate $mr = 0.2$ is taken and in iteration $t$ a number between 0 and 1 is randomly selected for each particle in group G1 ($X_j$ , $j$=1,..., $np/2$).

$$r_j(t) \in [0, 1] \tag{16}$$

$$X_j(t) = \{x_{j1}(t) \quad x_{j2}(t) \quad \cdots \quad x_{ji}(t) \quad \cdots \quad x_{jm}(t)\}^{\mathrm{T}} \tag{17}$$

For $j$th particle, if the selected random number is less than the mutation rate, one randomly selected component will be regenerated in the design space as follows

$$if\ r_j(t) \le mr \ \rightarrow \ x_{ji}(t) = x_{ji}^L + \mu(t) \times \left(x_{ji}^U - x_{ji}^L\right) \tag{18}$$

where $\mu$ is a random number in interval [0, 1] in iteration $t$; and $x_{ij}^L$ and $x_{ij}^U$ are lower and upper bounds of $x_{ji}$ in design space.

## 4. SEISMIC COLLAPSE SAFETY ASSESSMENT

The seismic collapse capacity of structures can be evaluated by the IDA-based methodology of FEMA-P695 [22]. In this methodology, nonlinear response-history analyses should be implemented for a suit of 22 ground motions of FEMA-P695. IDA curves are developed by recording maximum inter-story drift ratio, $ISD_{\mathrm{max}}$, versus the 5% damped spectral acceleration at structural fundamental period, $S_a(T_1$,5%$)$. Collapse margin ration (CMR) of structures is defined as the ratio of the spectral acceleration for which half of the pre-defined earthquake records cause collapse ($S_a^{50\%}$) to the spectral acceleration of the maximum considered earthquake (MCE) ground motion ($S_a^{\mathrm{MCE}}$) as follows:

$$CMR = \frac{S_a^{50\%}}{S_a^{\mathrm{MCE}}} \tag{19}$$

To account for the spectral shape of ground motion records, an adjusted collapse margin ration (ACMR) is defined as follows in which $SSF$ is the spectral shape factor [22].

$$ACMR = SSF \times CMR \tag{20}$$

Furthermore, to address the effect of different uncertainty sources in seismic collapse safety of structures the composite uncertainty parameter, $\beta_{TOT}$, should be determined.

Acceptable values of $ACMR$ for a single design and a design group are denoted in FEMA-P695 by $ACMR_{20\%}$ and $ACMR_{10\%}$, respectively. In other words, a single design can be considered of acceptable collapse safety when its $ACMR$ is greater than $ACMR_{20\%}$. In addition, for a group of desgins, if the average of their $ACMR$s is greater than $ACMR_{10\%}$ their colllapse safety is considered to be acceptable.

## 5. METHODOLOGY

In the current work, a methodology is presented to assess the impact of strong column-weak beam (SCWB) criterion on seismic collapse performance of optimally designed steel SMRF structures. The basic steps of the methodology are summarized below.

***Step1.*** Different values of 1.0, 1.25, 1.5, and 2.0 are taken for $FS$ in Eq. (1) based on the results of previous researches [4].

***Step2.*** For each value of $FS$, three independent PBD metaheuristic optimization runs are implemented with the aid of CMO algorithm. The obtain optimal designs of $X_1^*$ to $X_3^*$ are considered as a design group. In the PBD process, acceleration response spectra of the hazard levels are based on Iranian seismic design code [24] for soil type III in a very high seismicity region as shown in Fig. 1. hazard levels corresponding to 50%, and 2% probability of exceedance in 50 years, are denoted by 50/50 HL, and 2/50 HL, respectively. During the PBD optimization process, the structural seismic response is evaluated by performing pushover analysis based on the displacement coefficient method (DCM) of FEMA-356 [7].

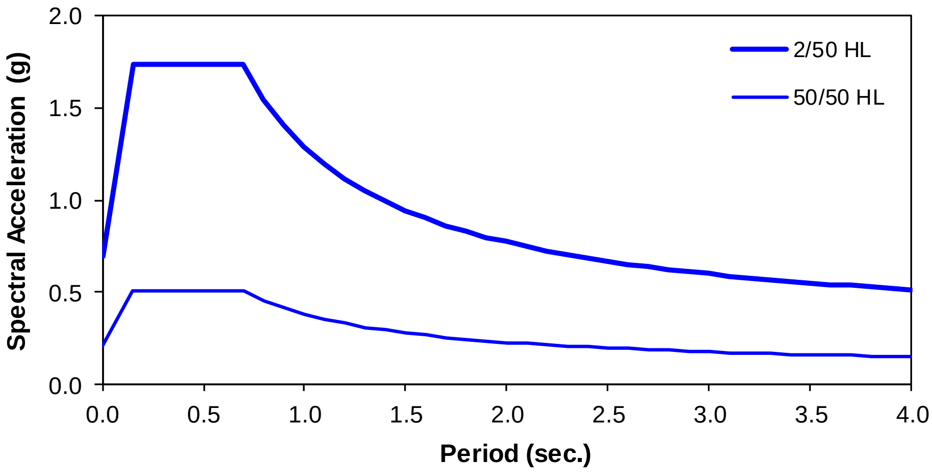

Figure 1. Acceleration response spectra of hazard levels

***Step 3.*** Seismic collapse capacity of the optimal designs $X_1^*$ to $X_3^*$ are evaluated based on the methodology of FEMA-P695. To compute the spectral acceleration of the MCE ground motion ($S_a^{\text{MCE}}$), the hazard model of Iranian seismic design code [24] is adopted. For the obtained optiml designs, $ACMR$ values are determined and compared with $ACMR_{20\%}$ and their average is compared with $ACMR_{10\%}$ to check the acceptability and feasibility of the optimal designs in terms of seismic collapse capacity. Based on the assumpations made in this work for uncertainty sources of record-to-record, design requirements, test data, and modeling, the values of $ACMR_{20\%}$ and $ACMR_{10\%}$ are 1.52 and 1.9, respectively. In addition, the effect of different values of SCWB ratios on optimal weight, confidence level and inter-story drifts of steel SMRFs are investigated.

## 6. NUMERICAL EXAMPLES

Fig. 2 shows the topology and member grouping details of three numerical examples of 5-, 10-, and 15-story steel SMRFs. The sections of all members are selected from the W-shaped sections listed in Table 1. The modulus of elasticity and yield stress are 210 GPa and 235 MPa, respectively. The constitutive law is bilinear with pure strain hardening slope of 3% of the elastic modulus. The dead and live loads of 2500 and 1000 kg/m are applied to the all beams, respectively.

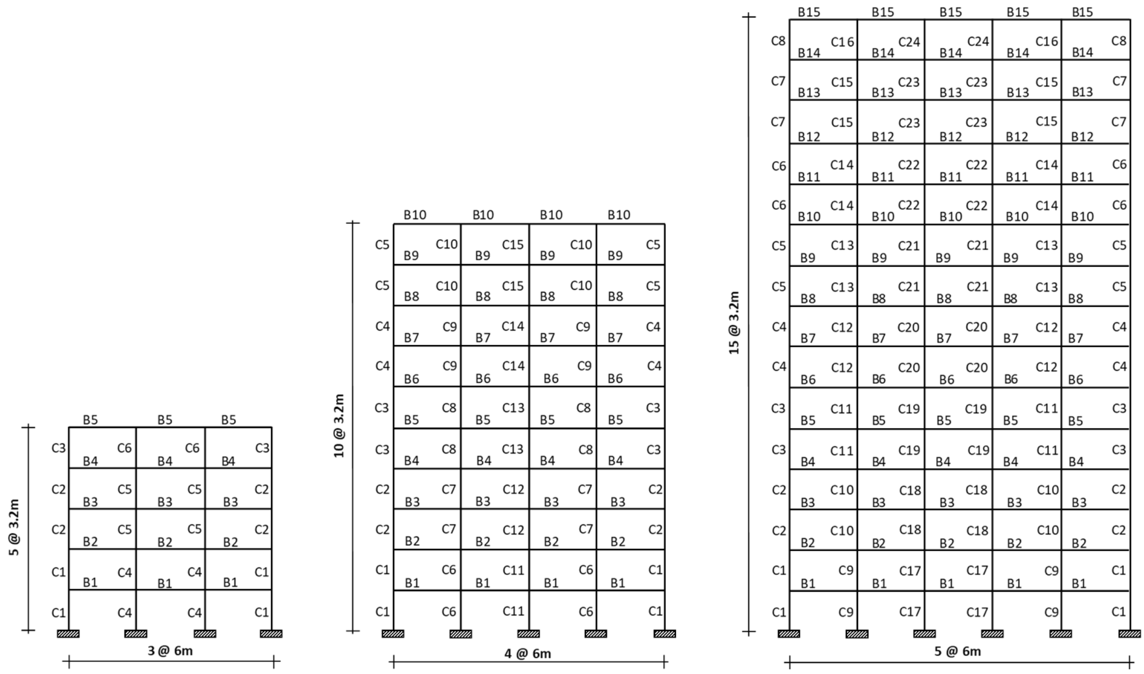


Figure 2. Topology and member grouping details of 5-, 10- and 15-story steel SMRFs

Table 1: Available W-shaped sections

| Columns | | | | Beams | | | |
|---|---|---|---|---|---|---|---|
| No. | Profile | No. | Profile | No. | Profile | No. | Profile |
| 1 | W14×48 | 13 | W14×257 | 1 | W12×19 | 13 | W21×50 |
| 2 | W14×53 | 14 | W14×283 | 2 | W12×22 | 14 | W21×57 |
| 3 | W14×68 | 15 | W14×311 | 3 | W12×35 | 15 | W24×55 |
| 4 | W14×74 | 16 | W14×342 | 4 | W12×50 | 16 | W21×68 |
| 5 | W14×82 | 17 | W14×370 | 5 | W18×35 | 17 | W24×62 |
| 6 | W14×132 | 18 | W14×398 | 6 | W16×45 | 18 | W24×76 |
| 7 | W14×145 | 19 | W14×426 | 7 | W18×40 | 19 | W24×84 |
| 8 | W14×159 | 20 | W14×455 | 8 | W16×50 | 20 | W27×94 |
| 9 | W14×176 | 21 | W14×500 | 9 | W18×46 | 21 | W27×102 |
| 10 | W14×193 | 22 | W14×550 | 10 | W16×57 | 22 | W27×114 |
| 11 | W14×211 | 23 | W14×605 | 11 | W18×50 | 23 | W30×108 |
| 12 | W14×233 | 24 | W14×665 | 12 | W21×44 | 24 | W30×116 |

*6.1 Example 1: The 5-story SMRF*

Three independent PBD optimization runs are performed for $FS = \{1.0 \quad 1.25 \quad 1.5 \quad 2.0\}$ and the best optimal design obtained in each case is given in Table 2. For these optimal designs the IDA and seismic collapse fragility curves are shown in Figs. 3 and 4, respectively. In addition, $ACMR$ of the optimal designs are reported in Table 2.

Table 2: PBOD best results for 5-story SMRF

| Design variables | *FS*=1.0 | *FS*=1.25 | *FS*=1.5 | *FS*=2.0 |
|---|---|---|---|---|
| C1 | W14×48 | W14×68 | W14×68 | W14×74 |
| C2 | W14×48 | W14×48 | W14×68 | W14×68 |
| C3 | W14×48 | W14×48 | W14×48 | W14×53 |
| C4 | W14×68 | W14×82 | W14×159 | W14×132 |
| C5 | W14×68 | W14×74 | W14×82 | W14×132 |
| C6 | W14×48 | W14×53 | W14×48 | W14×68 |
| B1 | W18×35 | W18×35 | W12×22 | W18×35 |
| B2 | W18×35 | W18×35 | W21×44 | W18×35 |
| B3 | W18×40 | W18×35 | W12×35 | W18×35 |
| B4 | W12×22 | W12×22 | W12×35 | W12×22 |
| B5 | W12×22 | W18×35 | W12×22 | W12×22 |
| Weight (kg) | 9470.22 | 10488.79 | 12334.71 | 12892.41 |
| $CL_{IO}$ (%) | 53.79 | 57.15 | 56.51 | 52.43 |
| $CL_{CP}$ (%) | 99.31 | 99.23 | 99.25 | 99.33 |
| $ACMR$ | 3.385 | 3.778 | 3.854 | 3.368 |

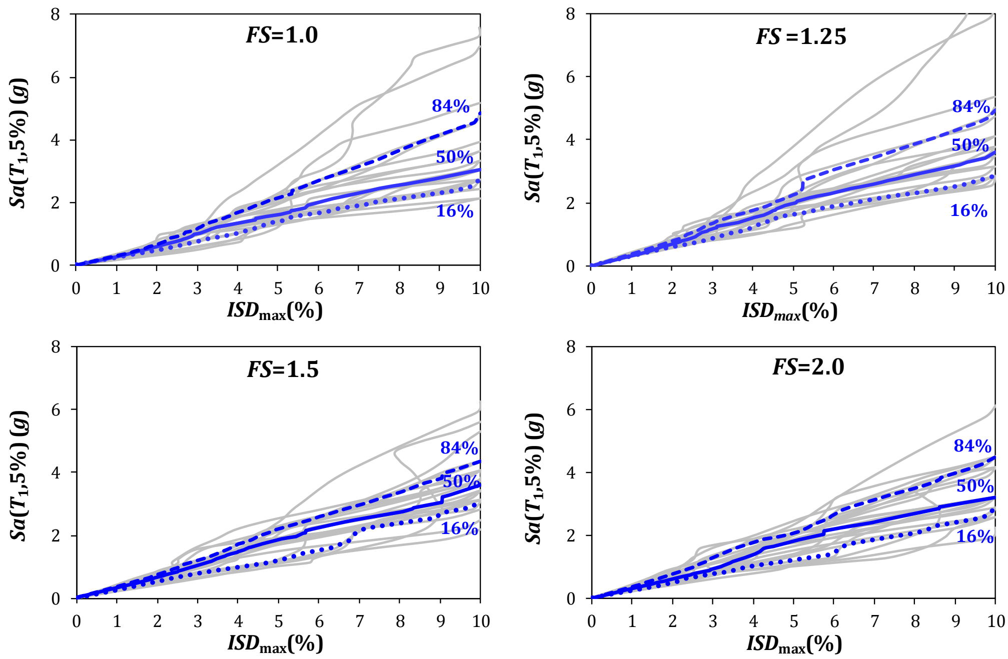


Figure 3. IDA curves for the best optimum 5-story SMRFs for different values of $FS$

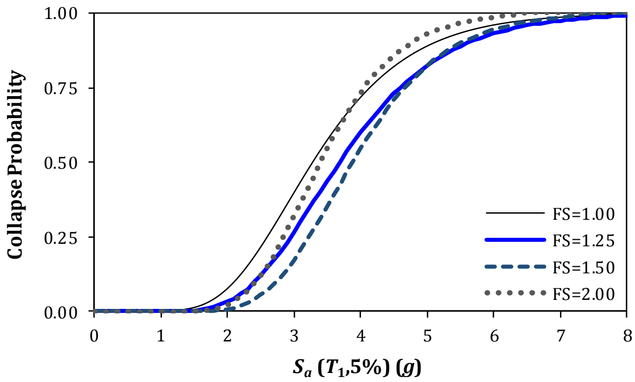


Figure 4. Fragility curves for the best optimum 5-story SMRFs for different values of $FS$

The structural weight of optimal design obtained for $FS$=2.0 is 36.14%, 22.92%, and 4.52% greater than those of $FS$=1.0, 1.25, and 1.5, respectively. While, $ACMR$ of this optimal design is 0.5%, 10.85%, and 12.61% less than the $ACMR$s of optimal designs attained by considering $FS$=1.0, 1.25, and 1.5, respectively.

$ACMR$s and optimal weights of three optimal designs obtained for each $FS$ are shown in Fig. 5. It can be observed that for $FS$=1.0, 1.25, and 1.5 the $ACMR$ is in increasing order and for $FS$=2.0 it is reduced. Moreover, the numerical results indicate that as $FS$ increases, the optimal weight increases. Because $ACMR$s of the optimal designs are greater than $ACMR_{20\%} = 1.56$ and the average of $ACMR$s shown in Fig. 5 are greater than $ACMR_{10\%} = 1.9$, it is rational to conclude that the best optimal designs for the 5-story SMRF may be found by taking $FS$=1.0.

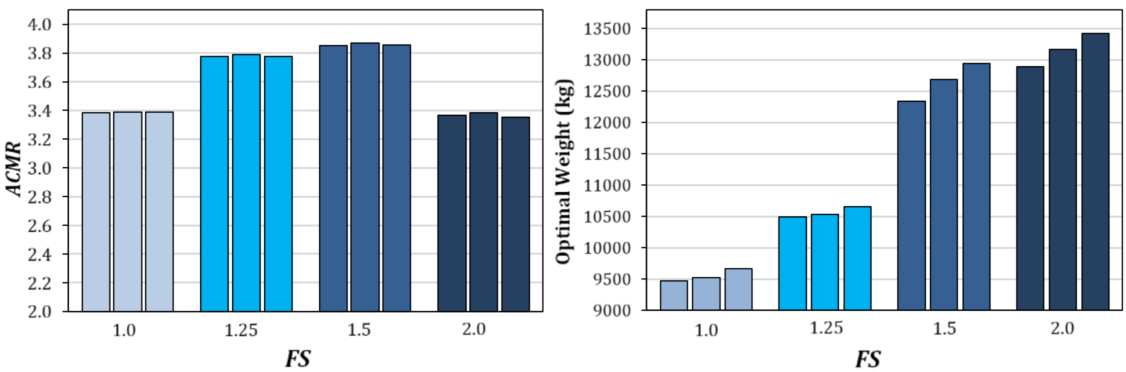


Figure 5. $ACMR$s and optimal weights of three optimal 5-story SMRFs for all values of $FS$

## *6.2 Example 2: The 10-story SMRF*

For 10-story SMRF, three independent seismic PBD optimization runs are performed for all values of $FS = \{1.0 \quad 1.25 \quad 1.5 \quad 2.0\}$ and the best obtained optimal designs are given in Table 3 together with their confidence levels at IO and CP levels. Furthermore, $ACMR$ of the optimal designs are reported in Table 3. For these optimal designs the IDA and seismic collapse fragility curves are shown in Figs. 6 and 7, respectively.

Table 3: PBOD best results for 10-story SMRF

| Design variables | $FS$=1.0 | $FS$=1.25 | $FS$=1.5 | $FS$=2.0 |
|---|---|---|---|---|
| C1 | W14×132 | W14×145 | W14×132 | W14×159 |
| C2 | W14×68 | W14×74 | W14×132 | W14×132 |
| C3 | W14×68 | W14×74 | W14×74 | W14×132 |
| C4 | W14×68 | W14×68 | W14×68 | W14×82 |
| C5 | W14×53 | W14×68 | W14×53 | W14×74 |
| C6 | W14×132 | W14×145 | W14×176 | W14×159 |
| C7 | W14×132 | W14×145 | W14×176 | W14×159 |
| C8 | W14×132 | W14×132 | W14×159 | W14×145 |
| C9 | W14×68 | W14×82 | W14×132 | W14×132 |
| C10 | W14×53 | W14×74 | W14×68 | W14×74 |
| C11 | W14×132 | W14×159 | W14×176 | W14×193 |
| C12 | W14×132 | W14×145 | W14×176 | W14×159 |
| C13 | W14×132 | W14×145 | W14×145 | W14×145 |
| C14 | W14×82 | W14×82 | W14×132 | W14×132 |
| C15 | W14×68 | W14×74 | W14×74 | W14×82 |
| B1 | W21×44 | W18×50 | W18×40 | W18×46 |
| B2 | W21×44 | W18×50 | W16×50 | W18×46 |
| B3 | W21×44 | W18×50 | W18×46 | W18×46 |
| B4 | W21×44 | W18×40 | W18×46 | W18×46 |
| B5 | W18×46 | W18×46 | W18×40 | W16×45 |
| B6 | W16×45 | W18×35 | W18×40 | W16×45 |
| B7 | W18×35 | W16×45 | W12×50 | W16×45 |
| B8 | W18×35 | W18×35 | W12×50 | W12×35 |
| B9 | W12×22 | W12×22 | W12×22 | W12×22 |
| B10 | W12×22 | W12×22 | W12×22 | W12×35 |
| Weight (kg) | 36125.73 | 39105.28 | 43508.57 | 45257.24 |
| $CL_{IO}$ (%) | 57.49 | 52.87 | 52.10 | 57.92 |
| $CL_{CP}$ (%) | 99.02 | 99.25 | 98.44 | 98.50 |
| $ACMR$ | 3.073 | 3.162 | 2.947 | 2.851 |

The structural weight of optimal 10-story design obtained for $FS$=2.0 is 25.28%, 15.73%, and 4.02% greater than those of $FS$=1.0, 1.25, and 1.5, respectively. While, $ACMR$ of this optimal design is 7.22%, 9.84%, and 3.26% less than the $ACMR$s of optimal designs attained by considering $FS$=1.0, 1.25, and 1.5, respectively. Fig. 8 presents $ACMR$s and optimal weights of three designs obtained for each $FS$ indicating that for each $FS$, $ACMR$s of the designs and their average are respectively greater than $ACMR_{20\%} =$ 1.56 and $ACMR_{10\%} =$ 1.9. Thus, by considering $FS$=1.0 the best design can be achieved for 10-story SMRF.

### *6.3 Example 3: The 15-story SMRF*

Table 4 reports the best optimal designs and their $ACMR$ values for 10-story SMRF. Figs. 9 and 10 show respectively the IDA and fragility curves of these designs.

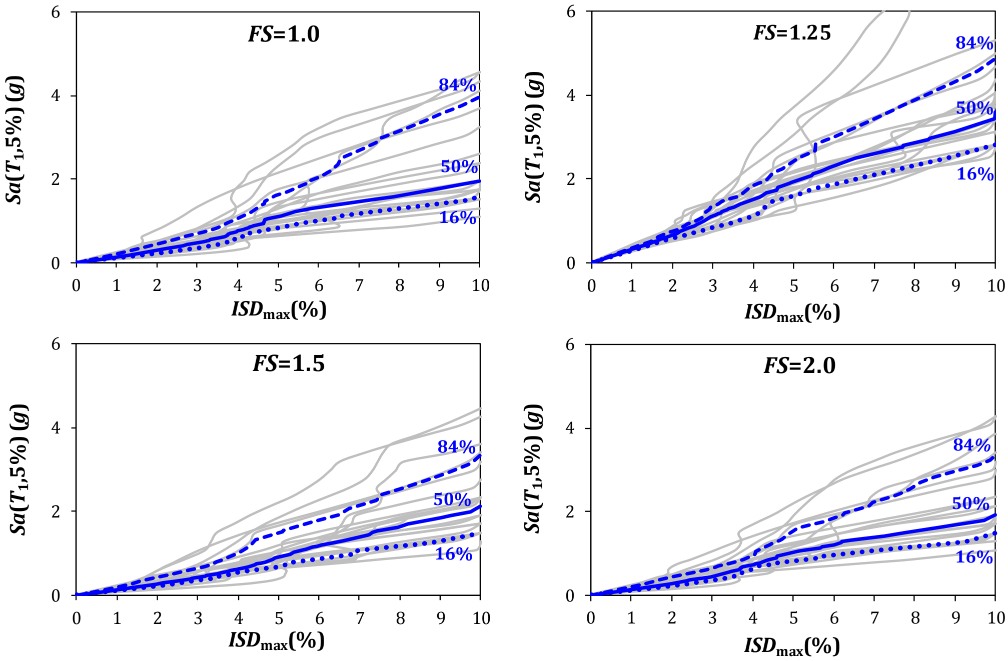


Figure 6. IDA curves for the best optimum 10-story SMRFs for different values of $FS$

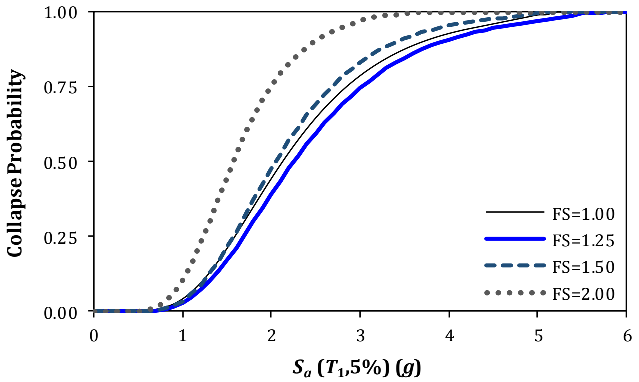


Figure 7. Fragility curves for the best optimum 10-story SMRFs for different values of $FS$

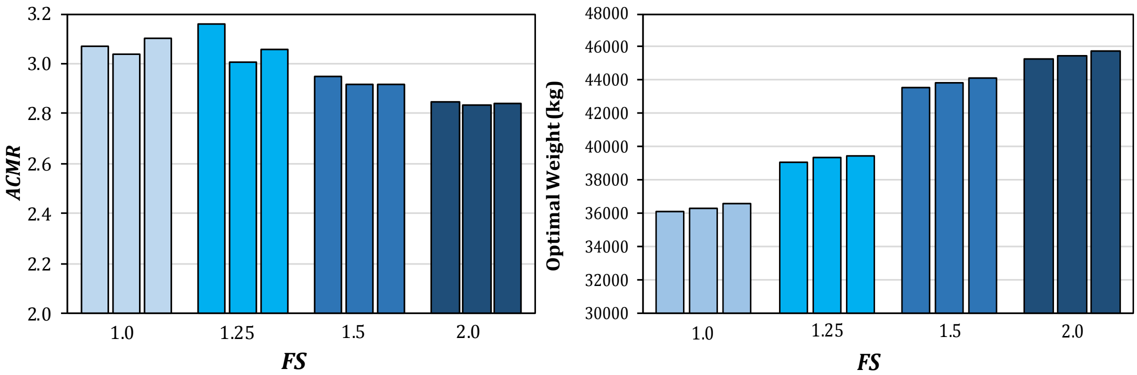


Figure 8. $ACMR$s and optimal weights of three optimal 10-story SMRFs for all values of $FS$

Table 4: PBOD best results for 15-story SMRF

| Design variables | $FS$=1.0 | $FS$=1.25 | $FS$=1.5 | $FS$=2.0 |
|---|---|---|---|---|
| C1 | W14×132 | W14×176 | W14x145 | W14×176 |
| C2 | W14×132 | W14×145 | W14×145 | W14×132 |
| C3 | W14×132 | W14×132 | W14×145 | W14×132 |
| C4 | W14×82 | W14×74 | W14×82 | W14×132 |
| C5 | W14×53 | W14×74 | W14×74 | W14×132 |
| C6 | W14×53 | W14×68 | W14×74 | W14×132 |
| C7 | W14×53 | W14×68 | W14×68 | W14×53 |
| C8 | W14×48 | W14×68 | W14×68 | W14×53 |
| C9 | W14×132 | W14×159 | W14×176 | W14×193 |
| C10 | W14×132 | W14×159 | W14×176 | W14×193 |
| C11 | W14×132 | W14×159 | W14×159 | W14×176 |
| C12 | W14×132 | W14×132 | W14×159 | W14×176 |
| C13 | W14×132 | W14×132 | W14×145 | W14×159 |
| C14 | W14×74 | W14×82 | W14×145 | W14×145 |
| C15 | W14×53 | W14×74 | W14×82 | W14×132 |
| C16 | W14×48 | W14×68 | W14×74 | W14×53 |
| C17 | W14×145 | W14×193 | W14×233 | W14×233 |
| C18 | W14×132 | W14×176 | W14×211 | W14×211 |
| C19 | W14×132 | W14×145 | W14×211 | W14×211 |
| C20 | W14×132 | W14×145 | W14×159 | W14×193 |
| C21 | W14×132 | W14×145 | W14×159 | W14×176 |
| C22 | W14×82 | W14×132 | W14×132 | W14×159 |
| C23 | W14×68 | W14×82 | W14×82 | W14×145 |
| C24 | W14×48 | W14×74 | W14×82 | W14×82 |
| B1 | W21×50 | W18×46 | W21×44 | W21×44 |
| B2 | W21×44 | W18×46 | W21×57 | W21×50 |
| B3 | W21×50 | W21×50 | W21×50 | W21×50 |
| B4 | W21×50 | W21×57 | W21×44 | W21×44 |
| B5 | W21×44 | W21×44 | W18×50 | W18×50 |
| B6 | W21×44 | W21×44 | W21×44 | W21×44 |
| B7 | W18×46 | W18×46 | W18×46 | W16×50 |
| B8 | W18×46 | W16×57 | W18×46 | W16×50 |
| B9 | W16×45 | W18×35 | W18×40 | W16×45 |
| B10 | W18×35 | W16×45 | W18×35 | W18×35 |
| B11 | W16×45 | W18×35 | W18×40 | W12×50 |
| B12 | W12×35 | W12×35 | W12×35 | W12×35 |
| B13 | W12×35 | W12×35 | W12×35 | W12×35 |
| B14 | W12×22 | W12×22 | W12×22 | W12×35 |
| B15 | W12×22 | W12×22 | W12×22 | W12×22 |
| Weight (kg) | 71621.84 | 81015.08 | 85864.45 | 95015.81 |
| $CL_{IO}$ (%) | 51.11 | 51.93 | 52.26 | 52.95 |
| $CL_{CP}$ (%) | 99.52 | 99.13 | 99.28 | 99.98 |
| $ACMR$ | 2.134 | 2.265 | 2.412 | 2.415 |

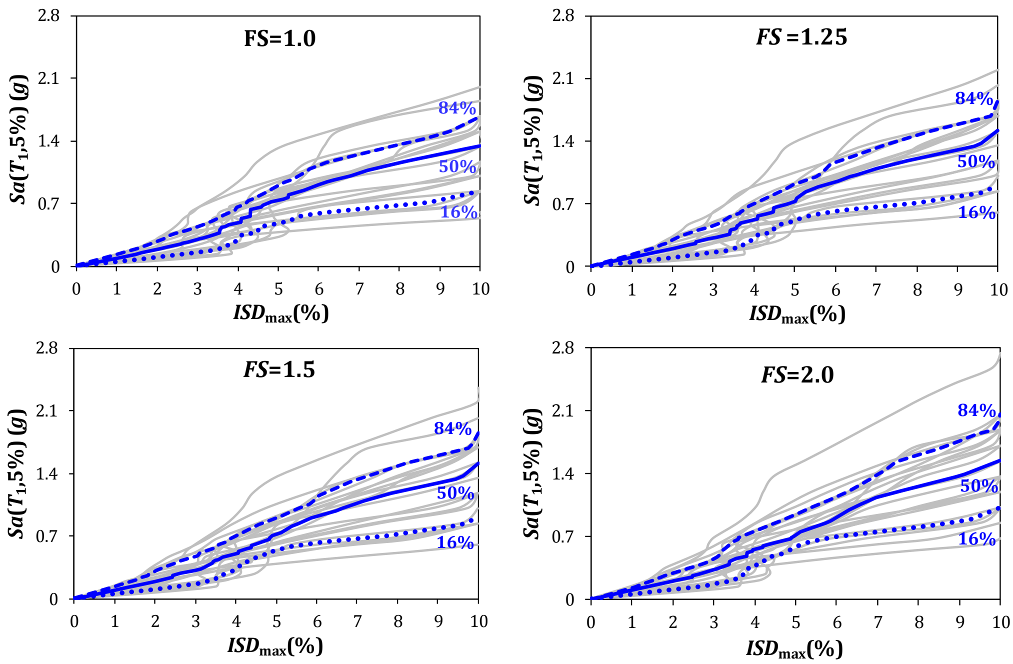


Figure 9. IDA curves for the best optimum 15-story SMRFs for different values of $FS$

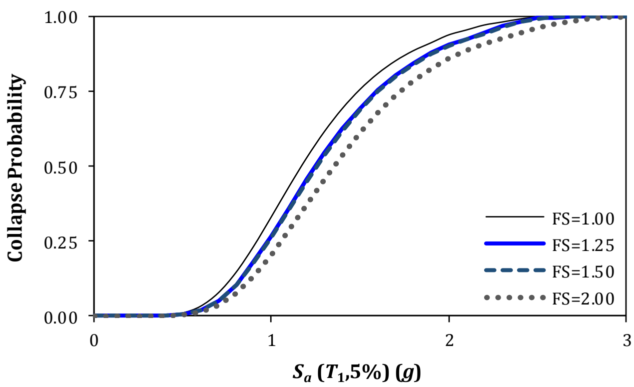


Figure 10. Fragility curves for the best optimum 15-story SMRFs for different values of $FS$

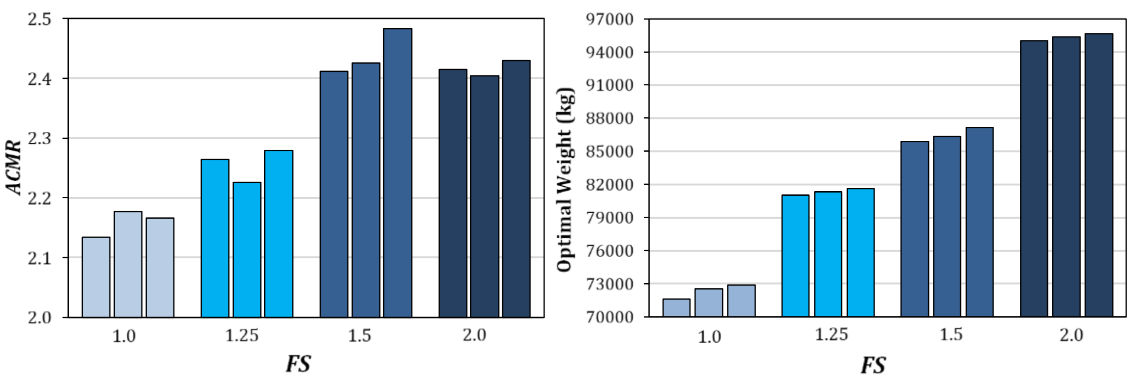


Figure 11. $ACMR$s and optimal weights of three optimal 15-story SMRFs for all values of $FS$

The weight of optimal design obtained for $FS$=2.0 is 32.66%, 17.28%, and 10.66% greater than those of $FS$=1.0, 1.25, and 1.5, respectively. While, $ACMR$ of this structure is 13.17%, 6.62%, and 0.12% greater than the $ACMR$ values of optimal designs obtained for $FS$=1.0, 1.25, and 1.5, respectively. $ACMR$s and optimal weights of three optimal designs obtained for each $FS$ are shown in Fig. 11. It can be observed that for each $FS$ value, $ACMR$ s and their average are greater than $ACMR_{20\%} = 1.56$ and $ACMR_{10\%} = 1.9$, respectively. Therefore, $FS$=1.0 is the best choice for 15-story SMRF.

## 7. CONCLUSIONS

In the current study, the effect of SCWB criterion on the seismic collapse performance of optimally designed SMRFs is evaluated. To achieve this task, different values for SCWB ratio, i.e. $FS = 1.0$, 1.25, 1.5, and 2.0, are considered and PBD optimization of SMRFs is implemented using COM metaheuristic algorithm. The design spectra of the Iranian seismic code 2800 are used to determine the hazard levels of interest. During the optimization process, the design constraints, including confidence levels in IO and CP performance levels, are checked according to FEMA-350 code. The seismic collapse capacity of the obtained optimal solutions is assessed based on the methodology of FEMA-P695 by performing IDA and generating seismic collapse fragility curves. Three design examples of 5-, 10-, and 15-story SMRFs are illustrated to investigate the efficiency of the proposed methodology. The results reveal that as $FS$ increases from 1.0 to 2.0, the optimal weight of SMRFs increases but $ACMR$ presents different behaviors in different examples. It is observed that in all the examples, $ACMR$ s of the optimal designs are greater than $ACMR_{20\%}$ and the average of $ACMR$s for each $FS$ are greater than $ACMR_{10\%}$. This means that all the PBD optimally designed SMRFs have acceptable seismic collapse performance. As the main finding of the present study, it is conclude that the best optimal designs for the SMRFs may be found by taking $FS$=1.0 in terms of economy and collapse performance.

## REFERENCES

1. Applied Technology Council (ATC), NEHRP seismic design technical brief no. 2 seismic design of steel special moment frames: a guide for practicing engineers. Report No. NIST GCR 09–917-3, Redwood City, CA, 2009.
2. AISC. Seismic provisions for structural steel buildings (ANSI/AISC 341-05), Chicago (IL): American Institute of Steel Construction, 2005.
3. Medina RA, Krawinkler H. Strength demand issues relevant for the seismic design of moment-resisting frames, *Earthq Spectra* 2005; **21**: 415-39.
4. Choi SW, Kim Y, Lee J, Hong K, Park HS. (2013). Minimumcolumn-to-beam strength ratios for beam-hinge mechanisms based on multi-objective seismic design, *J Constr Steel Res* 2013; **88**: 53–62.
5. Zaghi AE, Soroushian S, Itani A, Maragakis EM, Pekcan G, Mehrraoufi M. Impact of column-to-beam strength ratio on the seismic response of steel MRFs, *Bull Earthq Eng* 2015; **13**: 635-52.

6. Zareian F, Lignos DG, Krawinkler H. *Seismic Design Modification Factors for Steel Smrfs for Uniform Collapse Safety, Protection of the Built Environment Against Earthquakes*, Springer, New York, 2011.
7. FEMA-356, Prestandard and commentary for the seismic rehabilitation of buildings. Federal Emergency Management Agency, Washington, DC, 2000.
8. Fragiadakis M, Lagaros ND, Papadrakakis M. Performance-based multiobjective optimum design of steel structures considering life-cycle cost, *Struct Multidiscip Optim* 2006; **32**: 1–11.
9. Pan P, Ohsaki M, Kinoshita T. Constraint approach to performance-based design of steel moment-resisting frames, *Eng Struct* 2007; **29**: 186–94.
10. Kaveh A, Farahmand Azar B, Hadidi A, Rezazadeh Sorochi F, Talatahari S. Performance-based seismic design of steel frames using ant colony optimization, *J Constr Steel Res* 2010; **66**: 566–74.
11. Fragiadakis M, Lagaros ND. An overview to structural seismic design optimisation frameworks, *Comput Struct* 2011; **89**: 1155–65.
12. Kaveh A, Laknejadi K, Alinejad B. Performance-based multi-objective optimization of large steel structures, *Acta Mech* 2012; **232**: 355–69.
13. Kaveh A, Zakian P. Performance based optimal seismic design of RC shear walls incorporating soil–structure interaction using CSS algorithm, *Int J Optim Civil Eng* 2012; **2**: 383–405.
14. Liang JC, Li LJ, He JN. Performance-based multi-objective optimum design for steel structures with intelligence algorithms, *Int J Optim Civil Eng* 2015; **5**: 79–101.
15. Gholizadeh S. Performance-based optimum seismic design of steel structures by a modified firefly algorithm and a new neural network, *Adv Eng Softw* 2015; **81**: 50–65.
16. Rahami H, Mohebian P, Mousavi M. Performance-based connection topology optimization of unbraced and X-braced steel frames, *Int J Optim Civil Eng* 2017; **7**:451–68.
17. Ganjavi B, Hajirasouliha I. Optimum performance-based design of concentrically braced steel frames subjected to near-fault ground motion excitations, *Int J Optim Civil Eng* 2019; **9**:177–93.
18. Gholizadeh S, Ebadijalal M. Performance based discrete topology optimization of steel braced frames by a new metaheuristic, *Adv Eng Softw* 2018; **123**: 77–92.
19. Hassanzadeh A, Gholizadeh S. Collapse-performance-aided design optimization of steel concentrically braced frames, *Eng Struct* 2019; **197**:109411.
20. Gholizadeh S, Hassanzadeh A, Milany A, Ghatte HF. On the seismic collapse capacity of optimally designed steel braced frames, *Eng Comput* 2020. (in press)
21. Vamvatsikos D, Cornell CA. Incremental dynamic analysis, *Earthq Eng Struct Dynam* 2002; **31**: 491–514.
22. FEMA-P695. Quantification of building seismic performance factors. Washington (DC): Federal Emergency Management Agency, 2009.
23. FEMA-350. Recommended seismic design criteria for new steel moment-frame buildings. Washington (DC): Federal Emergency Management Agency, 2000.
24. Standard No. 2800. Iranian Code of Practice for Seismic Resistant Design of Buildings, Building and Housing Research Center, Tehran, 2014.